

Reduction of ablated surface expansion in pulsed-power-driven experiments using an aerosol dielectric coating

Cite as: Phys. Plasmas **26**, 070704 (2019); <https://doi.org/10.1063/1.5066231>

Submitted: 12 October 2018 . Accepted: 11 June 2019 . Published Online: 19 July 2019

M. Evans,  M. B. Adams, P. C. Campbell,  N. M. Jordan, S. M. Miller,  N. B. Ramey,  R. V. Shapovalov, J. Young, I. West-Abdallah,  J. M. Woolstrum,  R. D. McBride, and  P.-A. Gourdain

COLLECTIONS

 This paper was selected as Featured

 This paper was selected as Scilight



View Online



Export Citation



CrossMark

ARTICLES YOU MAY BE INTERESTED IN

[Enhancing cylindrical compression by reducing plasma ablation in pulsed-power drivers](#)
Physics of Plasmas **26**, 042706 (2019); <https://doi.org/10.1063/1.5086305>

[Review of pulsed power-driven high energy density physics research on Z at Sandia](#)
Physics of Plasmas **27**, 070501 (2020); <https://doi.org/10.1063/5.0007476>

[Design of dynamic screw pinch experiments for magnetized liner inertial fusion](#)
Physics of Plasmas **26**, 102702 (2019); <https://doi.org/10.1063/1.5120529>



Physics of Plasmas
Features in Plasma Physics Webinars

Register Today!

Reduction of ablated surface expansion in pulsed-power-driven experiments using an aerosol dielectric coating



Cite as: Phys. Plasmas **26**, 070704 (2019); doi: 10.1063/1.5066231

Submitted: 12 October 2018 · Accepted: 11 June 2019 ·

Published Online: 19 July 2019



View Online



Export Citation



CrossMark

M. Evans,¹ M. B. Adams,¹ P. C. Campbell,² N. M. Jordan,² S. M. Miller,² N. B. Ramey,² R. V. Shapovalov,¹ J. Young,¹ I. West-Abdallah,¹ J. M. Woolstrum,² R. D. McBride,² and P.-A. Gourdain¹

AFFILIATIONS

¹Department of Physics and Astronomy, University of Rochester, Rochester, New York 14627, USA

²Department of Nuclear Engineering and Radiological Sciences, University of Michigan, Ann Arbor, Michigan 48109, USA

ABSTRACT

The quality of warm dense matter samples created by magnetic compression can be largely affected by material ablation. When the ablated material carries currents, local instabilities can grow, which can lead to nonuniformities in the final magnetic pressure. Extending the previous work by Peterson *et al.* [Phys. Rev. Lett. **112**, 135002 (2014)], Awe *et al.* [Phys. Rev. Lett. **116**, 065001 (2016)], and Hutchison *et al.* [Phys. Rev. E **97**, 053208 (2018)], the experiments reported here demonstrate that the expansion of the ablated material can be significantly reduced by using a simple aerosol spray technique. Coating the current-carrying surfaces with a 30–60- μm layer of polyurethane reduced the expansion of the ablated material by a factor of 2 and eliminated material ejections from sharp corners. This technique, tested at the Michigan Accelerator for Inductive Z-Pinch Experiments pulsed power facility at the University of Michigan with currents up to 400 kA, could allow the production of homogeneous warm dense matter samples on pulsed-power drivers. Because of the simplicity of this method, this work brings forth an important contribution to pulsed-power-driven experiments designed to study nuclear fusion, material properties, and radiation science.

Published under license by AIP Publishing. <https://doi.org/10.1063/1.5066231>

The ablation of metallic surfaces^{1–4} can be problematic for experiments designed to compress matter uniformly using magnetic fields. Since the ablated material can carry unstable asymmetric current channels, the applied magnetic field pressure quickly loses uniformity. Ablation depends on the current density, the current rise time, the type of material carrying the current,⁵ the level of impurities in the material,⁶ the roughness of the material surface, the magnetic configuration driving the material compression,^{7,8} and processes such as the electrothermal instability (ETI).^{9,10} If the ablated material ionizes, then current channels will form within the ablated material; this can then lead to magnetohydrodynamic (MHD) instabilities, such as the magneto-Rayleigh-Taylor instability (MRTI). Both ETI and MRTI can be detrimental to the symmetry obtained in high convergence liner implosions,¹¹ including those used in equation-of-state (EOS) experiments,¹² and in magneto-inertial fusion concepts such as MagLIF.^{13,14} Recent experiments on the Z-facility have shown that electrothermal instabilities can be mitigated by coating the outer surface of a metal liner with a thin layer of dielectric material, such as polypropylene¹⁵ or Epon.¹⁶ In Ref. 16, the Epon coating, 70 μm thick, was applied to the liner surface by first casting a thick layer of Epon on the liner surface and then machining the Epon down to the desired thickness on a

diamond-tipped lathe. On smaller machines, such as Zebra, parylene-N was deposited onto the outer surface of a solid aluminum rod using a chemical vapor deposition process, allowing ETI growth to be characterized quantitatively.⁶

In this letter, we demonstrate experimentally that a thin coating of polyurethane (thickness 30–60 μm), deposited via an aerosol spray, can substantially reduce the expansion of the ablated material from metal surfaces and eliminate material ejection from sharp transitions along the metal surfaces. The experimental setup is shown in Fig. 1. The load is a simple 6061 aluminum rod, 1 mm in diameter, connected to two brass electrodes. The experiments were performed on the Michigan Accelerator for Inductive Z-Pinch Experiments (MAIZE),¹⁷ a Linear Transformer Driver¹⁸ (LTD) at the University of Michigan.

The primary diagnostic used in these experiments was a 12-frame shadowgraphy system.^{19,20} The system is composed of an Invisible Vision Ultra UHSi 12-frame intensified CCD camera, which is capable of recording images with a minimum exposure of 5 ns. A single 2-ns laser pulse (532 nm Nd:YAG) was passed through an optical cavity to create multiple collinear beams, where subsequent beams were separated in time by 15 ns and the intensity of each subsequent beam was reduced by $\sim 10\%$. These beams were synchronized to the exposure

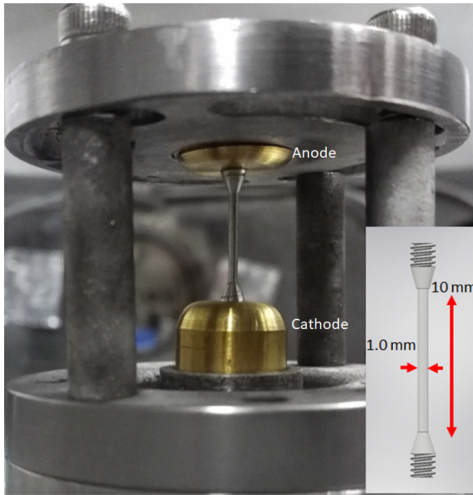


FIG. 1. Load hardware. The Al rod (1.0 mm diameter and 10 mm in height) screws into the top and bottom brass holders. The top threaded brass holder attaches rigidly to the anode, while the bottom brass holder has a slip-fit contact with the cathode.

times of the CCD camera to record 12 shadowgraphs per shot. Preshot images were used to establish the geometrical scale of each image, using the rod itself as both a scale-size reference and a spatial fiducial. Data from the shadowgraphs were used to obtain the time evolution of the ablated material.

These experiments were motivated by recent 2D (axial-radial) simulations of warm dense matter samples created by pulsed magnetic fields^{21,22} on mega-ampere drivers with fast (~ 100 ns) rise times²³ and by the findings of Peterson *et al.*¹⁵ These simulations suggested that a dielectric coating can tamp the expansion of the ablated material away from the surface of the material sample and thus greatly improve the uniformity of the implosion.

These experiments used “dumbbell” shaped load hardware to mitigate electrical arcing and nonthermal plasma creation at the main electrode contact points, following Awe *et al.*²⁴ The target assemblies were fabricated at the University of Rochester, in the eXtreme State Physics Laboratory. The Al rods, initially a 6–32 threaded rod stock, were machined down to a diameter of 1.0 ± 0.1 mm using a CNC lathe with a carbide bit. Conical sections connected the threaded ends of the rods to the central, 10-mm-long cylindrical section of the rods (see Fig. 1). The rod surfaces were not polished or quantitatively characterized, but they were smooth to the touch, and typical feature sizes for 6061 Al surfaces machined with carbide bits are expected to be in the range of 100–300 μm .²⁵ The lower brass dumbbell had an outer diameter of half an inch, and it was mated to the MAIZE cathode via a slip-fit connection. The upper dumbbell had an outer diameter of 9/16 in. and was threaded to rigidly attach to the upper anode plate on MAIZE. The 6–32 threaded Al rods were screwed into the brass holders, and the resulting target assembly was inserted into the anode-cathode structure on MAIZE. A single brass holder weighed approximately 10.7 g. The aluminum rod would stand upright without any bending when screwed into both brass holders. While the brass dumbbells survived the experiment, they were replaced after each experiment to limit shot-to-shot variations. The Al rods were destroyed in each shot.

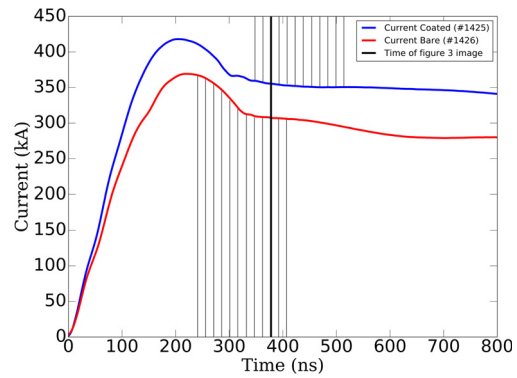


FIG. 2. Current trace for shot #1426 (red) and #1425 (blue). The thin vertical black lines indicate the image start times (laser pulse start times) for the 12-frame laser shadowgraphy system, where each frame was formed by a 2-ns laser pulse centered within a 5-ns CCD exposure. The thick vertical black line corresponds to the images presented in Fig. 3.

The dielectric coating was sprayed onto the rod, while the rod rotated on a lathe. Fast rotation limited clumping and drooling. The aerosol used was Minwax’s fast-drying polyurethane, which is an aliphatic hydrocarbon solvent mixture. The coating produced a reasonably uniform layer that was left to dry while rotating. The amount of coating was controlled simply by timing the application of the spray. The coating thickness was found by weighing the Al rod with a high precision scale (± 0.1 mg uncertainty) before and after applying the dielectric coating and assuming a uniform deposition along the length of the coating. The coating thickness for each rod was determined to be in the range of 30–60 μm .

This letter presents the results gathered from 10 shots performed at the MAIZE facility. The peak currents ranged from 260 kA to 425 kA (this large variation was due to the LTD misfiring). All shadowgraph images were taken well after peak current when the discharge current was decreasing (e.g., see Fig. 2). Note that when the discharge current decreases rapidly, the ablated material can expand rapidly into the surrounding vacuum region due to various phenomena such as the inverse skin effect.²⁶

The effect of the coating on the material expansion is clearly visible in the shadowgraphs shown in Fig. 3. To get a reasonable

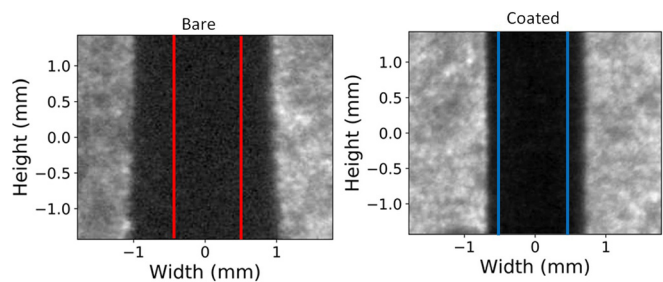


FIG. 3. Shadowgraph images of initially 1.0-mm diameter Al rods. Both images were taken at $t = 370$ ns. For the image on the right, the dielectric coating has a thickness between 30 and 60 μm . The colored lines illustrate the position of the outer surface of the bare rod (shot #1426) and the outer surface of the dielectric coating (shot #1425) prior to the shots.

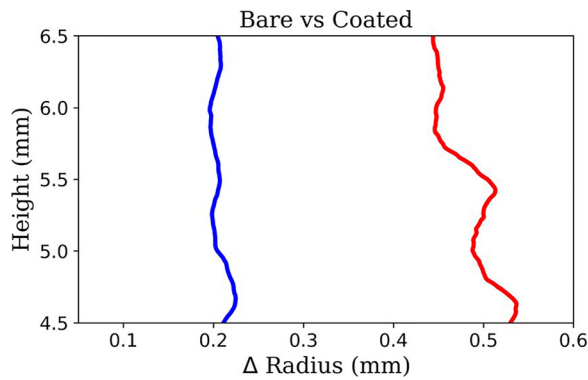


FIG. 4. Comparison of expansion between bare and coated Al rods at $t = 370$ ns. The blue trace is from the coated rod (shot 1425), and the red trace is from the bare rod (shot 1426).

quantitative measure of the expansion, a 2-mm axial length, centered on the rod midplane, was analyzed for each shadowgraph. Adaptive thresholding²⁷ was used to locate the material-vacuum interface. The original rod radius was subtracted at each axial location using the pre-shot images, which take into account a slight axial taper (~ 0.1 mm, larger at the bottom) caused by machining. The results of this analysis are presented in Fig. 4, which shows that (a) the expansion of the bare rod is more than twice the expansion of the coated rod at $t = 370$ ns; (b) the perturbation amplitude of the bare rod can reach approximately $50 \mu\text{m}$, while the amplitude of the coated rod remains below $20 \mu\text{m}$; and (c) there is a top-bottom asymmetry present in the bare case that is $\sim 100 \mu\text{m}$ (larger at the cathode), while the top-bottom asymmetry for the coated case is significantly less (if present at all).

The time evolution of the rod's expansion is plotted in Fig. 5 for both cases. The average expansion over a 2 mm length of the rod is shown for all 12 frames on the shadowgraphy system. The time evolution highlights two important effects. First, the coating has delayed the onset of material expansion by 74 ns. Second, the expansion of the coated rod appears to saturate at late times.

To study how the dielectric coating affects material expansion from sharp metal edges, a discontinuity was machined into the interface between the conical and straight sections of the rod. This sharp transition is shown in Fig. 6(b). The step edge was formed by machining away 0.1 mm from the conical section of the load.

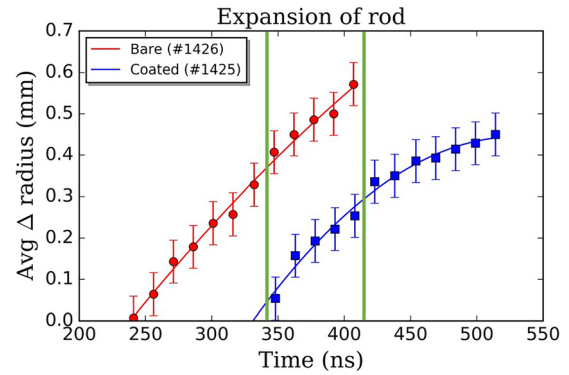


FIG. 5. Average expansion as a function of time. The red circles are the bare rod (shot 1426). The blue squares are the coated rod (shot 1425). Only the times that overlapped were compared (i.e., the times within the green vertical lines). Least squares polynomial fits to the data are also plotted.

Figures 6(a) and 6(c) show that the bare rod (shot 1416) and the coated rod (shot 1421) behave differently in the sharp transition region. Namely, material is ejected from the transition region in the case of the bare rod [Fig. 6(a)], while no material ejection is observed for the case of the coated rod [Fig. 6(c)]. Note that the 12-frame CCD camera records both the laser light for the shadowgraphy system and the light emitted from the rod itself (i.e., “self-emission”) and that some self-emission is visible in Fig. 6(a) but is absent in Fig. 6(c). In Fig. 6(a), the ejected material is brighter than other regions of the rod, appearing as a bright annulus in front of the dark rod silhouette. Assuming that the material rarefies as it expands radially outward, the fact that the ejected material is brighter than the rest of the rod indicates that the ejected material is also hotter than the rest of the rod.

The material ejected from the step edge expanded at 10 km/s from 300 ns to 425 ns, which is almost double the speed of the material expansion along the rest of the rod. Figure 6(c) shows that a dielectric coating can effectively quench the material ejection, though the coated rod does appear to expand slightly more around the step edge than along its straight section. In total, 5 shots were taken with the step edge. In all step-edge shots without a coating (3 shots), material ejection was observed from the step edge. In all step-edge shots with a coating (2 shots), material ejection was absent, demonstrating that the effect is reproducible.

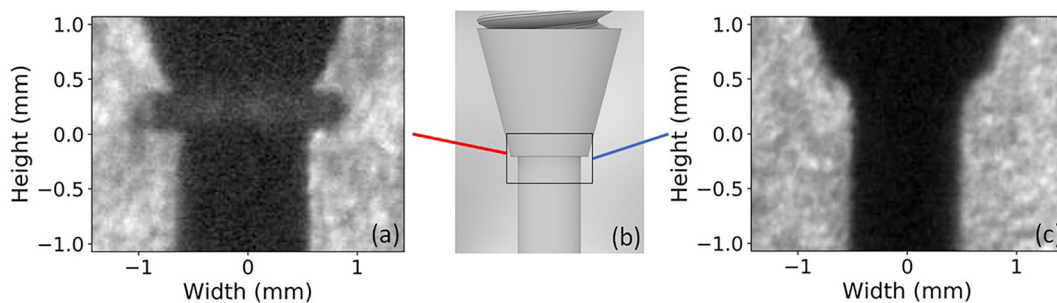


FIG. 6. (a) Ablation jet in the step edge region from an uncoated rod. (b) Zoomed-in view of the step edge in CAD software. (c) The coated rod with no visible material ejection from the step edge. Both shadowgraphs were taken at roughly ~ 360 ns; (a) was taken at 361 ns and (c) was taken at 357 ns.

Understanding and controlling the expansion caused by ablation is key to the success of many experiments using pulsed-power drivers, from magneto-inertial fusion to magnetic anvil cells. The research presented here shows that a thin (30–60 μm) dielectric coating sprayed directly onto a metallic surface reduces material expansion, compared to a bare metallic surface. The coating appears to delay the onset of material expansion, allowing time for the confining magnetic pressure to increase and further resist material expansion into the vacuum region. The coating was also shown to be remarkably effective at quenching material ejection from sharp corners on machined metal surfaces. This has profound consequences for pulsed-power-driven experiments. For example, electrode surfaces with rough features can simply be sprayed with a polyurethane coating to prevent material jetting. If the electrodes were left untreated, the resulting jets could lead to significant current and power loss, which is a significant concern in modern pulsed-power-driven experiments.^{28,29} Finally, this dielectric coating technique might also be effective on rough surfaces, like the ones obtained from selective laser sintering, allowing the use of 3D-printed metal targets on pulsed-power drivers.

The authors would like to thank Brandon Foy and Dan Mager for helpful technical discussions. This research was supported by the NSF/DOE Partnership in Basic Plasma Science and Engineering via DOE Office of Science, Fusion Energy Sciences Grant No. DE-SC0016252, and NSF Grant Nos. PHY-1725178 and PHY-1705418.

REFERENCES

- ¹S. V. Lebedev, I. H. Mitchell, R. Aliaga-Rossel, S. N. Bland, J. P. Chittenden, A. E. Dangor, and M. G. Haines, *Phys. Rev. Lett.* **81**, 4152 (1998).
- ²R. F. Benjamin, J. S. Pearlman, E. Y. Chu, and J. C. Riordan, *Appl. Phys. Lett.* **39**, 848 (1981).
- ³J. D. Douglass, S. A. Pikuz, T. A. Shelkovenko, D. A. Hammer, S. N. Bland, S. C. Bott, and R. D. McBride, *Phys. Plasmas* **14**, 012704 (2007).
- ⁴S. V. Lebedev, R. Aliaga-Rossel, S. N. Bland, J. P. Chittenden, A. E. Dangor, M. G. Haines, and I. H. Mitchell, *Phys. Plasmas* **6**, 2016 (1999).
- ⁵P. F. Knapp, S. A. Pikuz, T. A. Shelkovenko, D. A. Hammer, and S. B. Hansen, *Phys. Plasmas* **19**, 056302 (2012).
- ⁶T. M. Hutchinson, T. J. Awe, B. S. Bauer, K. C. Yates, E. P. Yu, W. G. Yelton, and S. Fuelling, *Phys. Rev. E* **97**, 053208 (2018).
- ⁷P. F. Knapp, J. B. Greenly, P.-A. Gourdain, C. L. Hoyt, M. R. Martin, S. A. Pikuz, C. E. Seyler, T. A. Shelkovenko, and D. A. Hammer, *Phys. Plasmas* **17**, 012704 (2010).
- ⁸M. R. Martin, C. E. Seyler, and J. B. Greenly, *Phys. Plasmas* **17**, 052706 (2010).
- ⁹A. H. Nelson and M. G. Haines, *Plasma Phys.* **11**, 811 (1969).
- ¹⁰M. G. Haines, *J. Plasma Phys.* **12**, 1 (1974).
- ¹¹M. G. Haines, *Plasma Phys. Controlled Fusion* **53**, 093001 (2011).
- ¹²R. W. Lemke, D. H. Dolan, D. G. Dalton, J. L. Brow, K. Tomlinson, G. R. Robertson, M. D. Knudson, E. Harding, A. E. Mattsson, J. H. Carpenter *et al.*, *J. Appl. Phys.* **119**(1), 015904 (2016).
- ¹³S. A. Slutz, M. C. Hermann, R. A. Versey, A. B. Sefkow, D. B. Sinars, D. C. Royang, K. J. Peterson, and M. E. Cuneo, *Phys. Plasmas* **17**, 056303 (2010).
- ¹⁴M. R. Gomez, S. A. Slutz, A. B. Sefkow, D. B. Sinars, K. D. Hahn, S. B. Hansen, E. C. Harding, P. F. Knapp, P. F. Schmit, C. A. Jennings *et al.*, *Phys. Rev. Lett.* **113**, 155003 (2014).
- ¹⁵K. J. Peterson, T. J. Awe, E. P. Yu, D. B. Sinars, E. S. Field, M. E. Cuneo, M. C. Herrmann, M. Savage, D. Schoen, K. Tomlinson, and C. Nakhleh, *Phys. Rev. Lett.* **112**, 135002 (2014).
- ¹⁶T. J. Awe, K. J. Peterson, E. P. Yu, R. D. McBride, D. B. Sinars, M. R. Gomez, C. A. Jennings, M. R. Martin, S. E. Rosenthal, D. G. Schroen, A. B. Sefkow, S. A. Slutz, K. Tomlinson, and R. A. Vesey, *Phys. Rev. Lett.* **116**, 065001 (2016).
- ¹⁷R. M. Gilgenbach, M. R. Gomez, J. C. Zier, W. W. Tang, D. M. French, Y. Y. Lau, M. G. Mazarakis, M. E. Cuneo, M. D. Johnston, B. V. Oliver, T. A. Melhorn, A. A. Kim, and V. A. Sinebryukhov, *AIP Conf. Proc.* **1088**, 259 (2009).
- ¹⁸A. A. Kim, M. G. Mazarakis, V. A. Sinebryukhov, B. M. Kovalchuk, V. A. Visir, S. N. Volkov, F. Bayol, A. N. Bostrikov, V. G. Durakov, S. V. Frolov, V. M. Alexeenko, D. H. McDaniel, W. E. Fowler, K. LeChien, C. Olson, W. A. Stygar, K. W. Struve, J. Porter, and R. M. Gilgenbach, "Development and tests of fast 1-MA linear transformer driver stages," *Phys. Rev. Spec. Top.—Accel. Beams* **12**, 050402 (2009).
- ¹⁹D. A. Yager-Elorriaga, P. Zhang, A. M. Steiner, N. M. Jordan, Y. Y. Lau, and R. M. Gilgenbach, *Phys. Plasmas* **23**, 101205 (2016).
- ²⁰P. C. Campbell, J. M. Woolstrum, F. Antoulakis, T. M. Jones, D. A. Yager-Elorriaga, S. M. Miller, N. M. Jordan, Y. Y. Lau, R. M. Gilgenbach, and R. D. McBride, *IEEE Trans. Plasma Sci.* **46**, 3973–3981 (2018).
- ²¹P. Gourdain, A. B. Sefkow, and C. E. Seyler, "The generation of warm dense matter using a magnetic anvil cell," *IEEE Trans. Plasma Sci.* **46**, 3968 (2018).
- ²²P.-A. Gourdain, M. B. Adams, M. Evans, H. R. Hasson, R. V. Shapovalov, J. R. Young, and I. West-Abdallah, "Enhancing cylindrical compression by reducing plasma ablation in pulsed-power drivers," *Phys. Plasmas* **26**, 042706 (2019).
- ²³P.-A. Gourdain, *IEEE Trans. Plasma Sci.* **43**, 2547 (2015).
- ²⁴T. J. Awe, B. S. Bauer, S. Fuelling, I. R. Lindemuth, and R. E. Siemon, *Phys. Plasmas* **17**, 102507 (2010).
- ²⁵F. Colvin and R. LeGrand, *The New American Machinist's Handbook* (McGraw-Hill, New York, 1955).
- ²⁶M. G. Haines, *Proc. Phys. Soc.* **74**, 576 (1959).
- ²⁷See <https://opencv-python-tutorials.readthedocs.io> for a tutorial about using OpenCV for 2D image processing.
- ²⁸A. Porwitzky and J. Brown, *Phys. Plasmas* **25**, 063102 (2018).
- ²⁹A. Porwitzky, D. H. Dolan, M. R. Martin, G. Laity, R. W. Lemke, and T. R. Mattsson, *Phys. Plasmas* **25**, 063110 (2018).